Orbits and fields in the helical wiggler

John P. Blewett and R. Chasman

Citation: Journal of Applied Physics **48**, 2692 (1977); doi: 10.1063/1.324119
View online: http://dx.doi.org/10.1063/1.324119
View Table of Contents: http://scitation.aip.org/content/aip/journal/jap/48/7?ver=pdfcov
Published by the AIP Publishing

Orbits and fields in the helical wiggler*

John P. Blewett and R. Chasman

Brookhaven National Laboratory, Upton, New York 11973
(Received 24 May 1976; accepted for publication 3 January 1977)

The "helical wiggler" is a device in which relativistic electrons pass through a transverse magnetic field whose direction revolves with distance along the beam axis. In this paper we discuss the electron orbits in this device. The field patterns and necessary current distributions are established. Finally, the question is treated as to whether this device can be incorporated into a storage ring without destroying the circulating beam. It is concluded that there is reason to expect satisfactory performance from helical wigglers in storage rings.

PACS numbers: 41.70.+t, 41.80.Dd, 29.20.Dh, 41.10.Dq

I. INTRODUCTION

In a recent publication Elias *et al.*[1] describe the "observation of stimulated emission of radiation by relativistic electrons in a spatially periodic transverse magnetic field". The observed radiation is a phenomenon predicted several years ago by Motz[2] and analyzed by Purcell (in unpublished reports) and by Madey.[3] The earlier papers considered only radiation induced on passage of electrons through a magnetic field whose direction is periodically reversed. Madey's paper and the paper of Elias *et al.* describe radiation induced in a transverse magnetic field whose direction revolves around the beam axis. The experiment described in Ref. 1 used a linear accelerator beam which made a single passage through the device. The possibility of incorporation of a spiralling transverse magnetic field in a storage ring to yield a radiation spectrum more sharply peaked than the usual synchrotron radiation spectrum has recently been recognized by Kincaid.[4] His paper appears as a companion paper to this one (preceding paper).

The radiation under discussion is essentially synchrotron radiation emitted when electrons travel on a helical path through a spiralling transverse magnetic field. When the electron orbit makes many turns in the spiralling field the radiation spectrum, heavily affected by Lorentz transformations, peaks at a wavelength roughly γ^{-2} times the period of the spiralling magnetic field. In the Stanford study (Elias *et al.*[1]) the period of the spiralling field was 3.2 cm. Electrons of energy 24 MeV passed through the field pattern which was applied over a distance of 5.2 m along the electron orbit. The transverse field on axis was 2300 G. Radiation was observed at the predicted frequency of 10.6 μ.

Since the radiation in this system is much more nearly monochromatic than the radiation from electrons in a storage ring or synchrotron, it is of considerable interest to consider inclusion of a spiralling transverse field system in a storage ring built as a dedicated source of synchrotron radiation. In this paper the field patterns and electron orbits in the spiralling field system are explored and the implications for incorporating it in a storage ring are derived.

At Stanford, the device is referred to as a "free electron laser". Synchrotron radiation specialists describe it as a "helical wiggler".

II. DESCRIPTION OF MAGNET SYSTEM

The spiralling field pattern is produced by a double-helix bifilar magnet which can be visualized if one assumes that on the outside of a bore tube an open helix is wound, and then a second helix is wound in the spaces between turns of the first helix. When currents in opposite directions are passed through the two helices, the central axial magnetic field is cancelled and the spiralling transverse field pattern appears.

If the helices consist of wires of infinitesimal cross section, the field pattern on axis can be derived as a function of current in the helices. The result for a single open helix is given by Smythe[5] and is derived for the double helix by Kincaid.[4]

III. FIELD AND CURRENT DISTRIBUTIONS

It will be assumed that the field pattern has a sinusoidal variation in the axial direction and that no higher harmonics are present.

The magnetic field patterns and current distributions in the magnet system are derived in the Appendix. The fields to be traversed by the electron beam are given

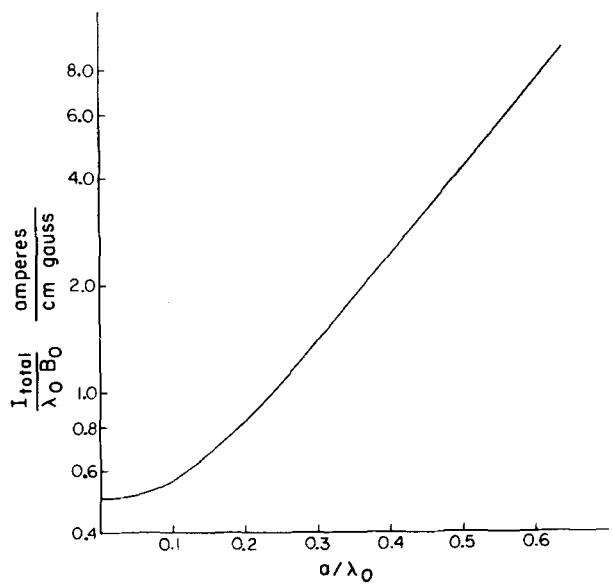

FIG. 1. Current I_{tot} per turn required to produce an axial transverse field B_0 in a helix of pitch λ_0 as a function of the ratio of helix radius to pitch.

by

$$B_r = 2B_0[I_0(kr) - (i/kr)I_1(kr)]\sin(\theta - kz),$$
$$B_\theta = (2B_0/kr)I_1(kr)\cos(\theta - kz), \quad (1)$$
$$B_z = -2B_0 I_1(kr)\cos(\theta - kz),$$

where B_0 is the transverse field amplitude at the axis of the system, I_0 and I_1 are Bessel functions, and $k = 2\pi/\lambda_0$ where λ_0 is the pitch of the helical winding.

Near the axis the Bessel functions can be approximated by expressions given in the Appendix.

The current in the helical winding required to produce a transverse field B_0 on the axis of a helix of pitch λ_0 is plotted as a function of the ratio of helix radius to pitch in Fig. 1.

IV. ELECTRON ORBITS

The analysis which follows has been guided by computer runs which have indicated the character of the orbits. The computer runs have traced electrons under various conditions through the fields described by Eqs.(1). It has thus been established that the orbit includes oscillations at three main frequencies. The primary motion is helical with an orbit radius of a small fraction of a millimeter. The period of the motion is the same as that of the transverse field and its axis oscillates around the physical axis of the helix with a much lower frequency. At a still lower frequency the x and y components of the intermediate-frequency oscillation couple to each other and exchange energy. The reasons for this behavior and the important parameters can be established by an approximate solution of the equations of motion.

An important simplification is possible when it is realized that excursions from the axis are small and that the major velocity component is the paraxial one. Since all applications will use highly relativistic electrons it is legitimate to set $\dot{z} = c$ and $z = ct$. This reduces to two the number of equations of motion which must be solved.

First, we shall establish the radius r_0 of the helical orbit. The field patterns (1), for the regions close to the axis, can be approximated by

$$B_r = B_0\sin(\theta - kct),$$
$$B_\theta = B_0\cos(\theta - kct), \quad (2)$$
$$B_z = 0.$$

It is easy to show that the helical orbit through these fields has

$$\dot{\theta} = kc,$$
$$r = r_0 = 1/k^2\rho,$$

where ρ $(= m_0\gamma c/eB_0)$ is the cyclotron radius in the field B_0.

When the lower-frequency oscillation has carried the helical orbit some distance from the axis, the amplitudes of B_r and B_θ, given by Eqs. (1), are no longer equal and the projection of the helical orbit on the r-θ plane is no longer exactly circular. Its average value will, however, be given by solution of the following equation (expressed in a coordinate system having its origin on the instantaneous axis of the helix):

$$mr\dot{\theta}^2 = -er\dot{\theta}B_z + e\dot{z}B_t, \quad (3)$$

where B_t represents the transverse field which will alternate between B_r and B_θ (of the original coordinate system). From Eqs. (1) its average value will be $B_0 I_0(kR)$, where R is the displacement of the instantaneous axis of the helix from the central axis of the wiggler. Now, setting $\dot{\theta}$ again equal to kc and neglecting the small contribution of the B_z term in Eq. (3), we obtain

$$r_0 = I_0(kR)/k^2\rho. \quad (4)$$

Using the parameters of the Stanford experiment[1] ($k = 196$ m^{-1}, $\rho = 0.348$ m), we find for $R = 0$, $r_0 = 0.075$ mm. As will be shown later, the Stanford parameters with no initial correction lead to a "betatron oscillation" with an amplitude of about 6 mm. At the maximum excursion in this oscillation the value of r_0 is about 0.10 mm. These figures are in good agreement with those obtained from the computer runs.

To derive the characteristics of the lower-frequency oscillations it is necessary to solve the equations of motion

$$\ddot{x} = (e/m)(\dot{y}B_z - cB_y),$$
$$\ddot{y} = (e/m)(cB_x - \dot{x}B_z). \quad (5)$$

We substitute for B_x, B_y, and B_z expressions (A3) and we make the following substitution for x and y:

$$x = r_0\cos kct + u,$$
$$y = r_0\sin kct + v. \quad (6)$$

In making the substitution we note the fact that kr_0 is of the order of 0.01 when the Stanford parameters are used and is even smaller for higher-energy electrons. Accordingly, it is legitimate to neglect $k^2r_0^2$ with respect to unity. Assuming that u and v are slowly varying compared to $\cos kct$, one can write from Eqs. (5) and (6)

$$\ddot{u} + 2\delta\dot{v} + \omega^2 u = 0,$$
$$\ddot{v} - 2\delta\dot{u} + \omega^2 v = 0, \quad (7)$$

where

$$\delta = (kcr_0/2\rho)[1 + \tfrac{1}{4}k^2(u^2 + v^2)],$$
$$\omega^2 = (k^2c^2r_0/2\rho)[1 + \tfrac{1}{8}k^2(u^2 + v^2)]. \quad (8)$$

Solving Eqs. (7), taking into account the fact that δ is small compared with ω, we find that u and v are combinations of trigonometric functions of $\omega \pm \delta$. The coefficients of the functions will be determined by initial conditions. The values of u and v are

$$u = (x_0 - r_0)\cos\omega t\cos\delta t + \omega^{-1}[\delta x_0 - v_y + r_0(kc - \delta)]$$
$$\times\sin\omega t\sin\delta t + \omega^{-1}(\delta y_0 + v_x)\sin\omega t\cos\delta t - y_0\cos\omega t\sin\delta t, \quad (9)$$

$$v = \omega^{-1}[v_y - \delta x_0 - r_0(kc - \delta)]\sin\omega t\cos\delta t + (x_0 - r_0)$$
$$\times\cos\omega t\sin\delta t + y_0\cos\omega t\cos\delta t + \omega^{-1}(\delta y_0 + v_x)\sin\omega t\sin\delta t, \quad (10)$$

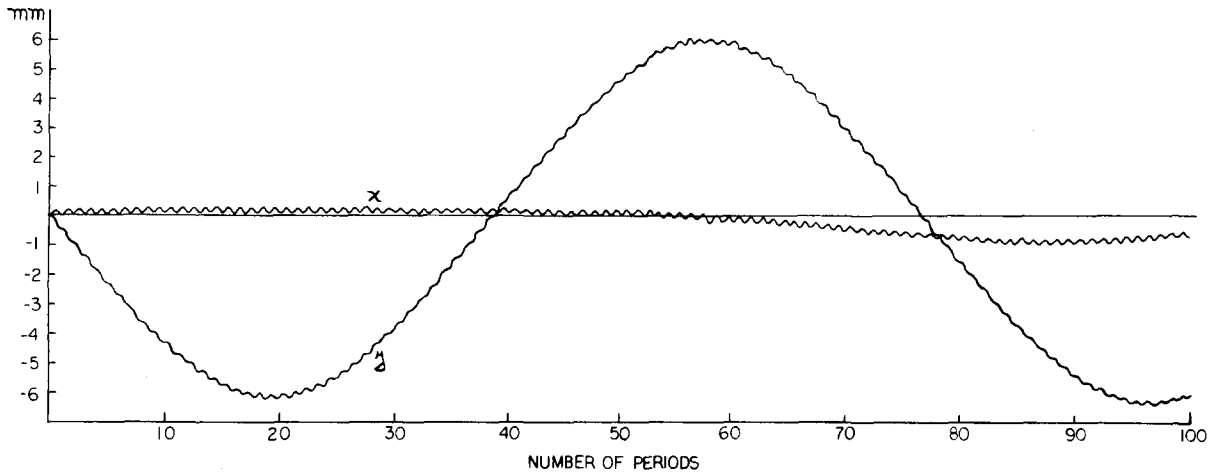

FIG. 2. Orbit in a helical wiggler with zero initial coordinates and transverse velocities.

where x_0, y_0, v_x, and v_y are the initial values of $x, y, \dot{x}$, and $\dot{y}$. Using the Stanford parameters we find that δ is of the order of 1% of ω which, in turn, is of the order of 1% of kc. Neglecting small terms and setting all of the initial parameters equal to zero, we obtain

$$x = r_0(t)\cos kct + [kcr_0(t=0)/\omega]\sin\omega t \sin\delta t, \tag{11}$$

$$y = r_0(t)\sin kct - [kcr_0(t=0)/\omega]\sin\omega t \cos\delta t. \tag{12}$$

For zero initial conditions, there will be a "betatron oscillation" with an amplitude of the order of one hundred times the radius of the basic helical motion r_0 and with a frequency of the order of 1% of that of the basic helical motion.

We turn now to establishing the values of the lower oscillation frequencies. First we use Eq. (4) to establish an average value of r_0. From Eqs. (6), (9), and (10)

$$R^2 \approx u^2 + v^2 \quad \text{(assuming } u \text{ and/or } v \text{ is much larger than } r_0\text{)}$$

$$= R_0^2 \sin^2(\omega t + \varphi),$$

where R_0 is the maximum excursion at the intermediate frequency. R_0 and φ are determined by the initial conditions.

From Eq. (4),

$$r_0 \approx (k^2\rho)^{-1}[1 + \tfrac{1}{4}k^2R_0^2\sin^2(\omega t + \varphi)].$$

Hence the average value of r_0 is

$$r_{0,\mathrm{av}} = (k^2\rho)^{-1}(1 + \tfrac{1}{8}k^2R_0^2).$$

Applying the same procedures to Eq. (10),

$$\omega^2 = (c^2/2\rho^2)(1 + \tfrac{1}{8}k^2R_0^2)(1 + \tfrac{1}{16}k^2R_0^2)$$

$$\omega = (0.707\ c/\rho)(1 + \tfrac{3}{32}k^2R_0^2),$$

$$\delta = (c/2k\rho^2)(1 + \tfrac{1}{4}k^2R_0^2).$$

Inserting the Stanford parameters, after a few algebraic manipulations the parameters prove to be

$$R_0 = 6.0\times10^{-3}\ \mathrm{m},$$

$$\omega = 7.4\times10^{8}\ \mathrm{sec}^{-1},$$

$$\delta = 1.0\times10^{7}\ \mathrm{sec}^{-1}.$$

For comparison, $kc = 5.9\times10^{10}\ \mathrm{sec}^{-1} = 80\omega$.

The results of the computer runs using the correct

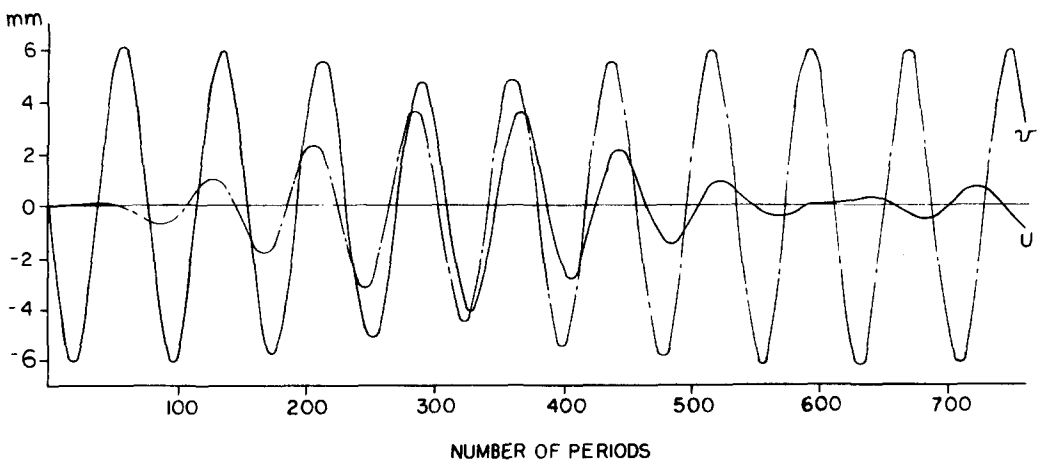

FIG. 3. The functions u and v in a very long wiggler.

field expressions (1) are shown in Figs. 2 and 3 for the case of zero initial conditions. Figure 2 shows the first 100 periods of the helical oscillation; Fig. 3 shows the behavior of u and v over an impractically long wiggler having over 700 periods. The results are in good agreement with the approximate theory outlined above. The value of ω is 7.6×10^8 to be compared with the predicted value of 7.4×10^8. The predicted value for the oscillation amplitude was 6.0 mm, to be compared with the correct value of 6.2 mm. The hypothetical computed wiggler was not long enough to establish the value of δ but evidently the predicted value is of the right order of magnitude.

V. EFFECT OF A SUPERPOSED AXIAL FIELD

In the Stanford experiment a 1000-G axial field was superposed on the wiggler field pattern by addition of a solenoid which enclosed the wiggler. Such a field can have marked effects both on the helical motion and on the betatron oscillation frequency and amplitude.

The wavelength of the helical motion will remain the same as the axial period of the helical winding. But the value of r_0, obtained from Eq. (3), will change if the axial field is strong enough that the first term on the right-hand side of Eq. (3) no longer can be neglected. Equation (3) then yields

$$r_0=\frac{I_0(kr)}{k^2\rho(1\pm 1/k\rho_1)}, \tag{13}$$

where ρ_1 $(=mc/eB_1)$ is the cyclotron radius in the added axial field B_1. In a field of 10 kG the added term will make a change of about 6% in the value of r_0. Whether r_0 is increased or decreased depends on the direction of the applied field.

To find the effect of the applied field on the betatron oscillations we reexamine Eqs. (7) and (8). Equation (7) will have the same form but it will be found that the expression for δ is changed to

$$\delta=(kcr_0/2\rho)[1+\tfrac{1}{4}k^2(u^2+v^2)]\pm c/2\rho_1. \tag{14}$$

Here, as before, the choice of plus or minus sign depends on the direction of the applied field. If the applied field B_1 is of the same order as B_0, then, since kr_0 is small (of the order of 10^{-2}) the new term is the only significant one. The expression for ω^2 is unchanged but now δ is of the same order as ω and terms in δ/ω no longer can be neglected. Equations (7) now yield for the frequency of the betatron oscillation the quantity

$$[\omega^2+2\delta^2\pm 2\delta(\omega^2+\delta^2)^{1/2}]^{1/2}. \tag{15}$$

For small-amplitude betatron oscillations where k^2u^2 and k^2v^2 are negligible compared with unity, (15) becomes

$$kc\left\{\frac{1}{2}\left(\frac{r_0}{\rho}+\frac{1}{k^2\rho_1^2}\right)\pm\frac{1}{k\rho_1}\left[\frac{1}{2}\left(\frac{r_0}{\rho}+\frac{1}{2k^2\rho_1^2}\right)\right]^{1/2}\right\}^{1/2}. \tag{16}$$

For applied axial fields of 1, 5, and 10 kG the two frequencies f_1 and f_2 given by Eq. (16) are (using the Stanford parameters)

B_1 (kG)	f_1 (sec^{-1})	f_2 (sec^{-1})
1	8.2×10^8	4.5×10^8
5	20.5×10^8	1.8×10^8
10	38.4×10^8	1.0×10^8.

The oscillation no longer has the same character as that produced only by the wiggler but is the sum of sines and cosines of the two frequencies with amplitudes determined by initial conditions. The overall oscillation amplitudes are smaller than before and can be reduced to negligible levels by suitable choices of initial conditions.

VI. PRACTICAL CONSIDERATIONS

Several practical problems remain to be solved before the helical wiggler can be incorporated into a storage ring.

First, a reasonable end configuration must be designed and the end field pattern studied. During our computer studies we have introduced a tapered field pattern at the end, maintaining the same period of the helical field pattern. Orbits through this pattern were not notably different from the orbits in the wiggler with discontinuous ends. It appears impractical to taper the end fields so slowly that the entry and exit behavior can be considered adiabatic.

Second, such large oscillations as those predicted for zero initial conditions cannot be tolerated. Magnetic kicks must be introduced at the entrance to reduce the betatron oscillations to negligible amplitudes and at the exit to restore the electrons to the equilibrium orbit of the storage ring. Such kicks have been introduced in the computer program; as predicted by Eq. (12) an initial v_y of approximately kcr_0 is required. This is entirely effective in reducing the radial excursions to fractions of a millimeter. The initial deflection required for the parameters considered was about 20 mrad. Figure 4 shows the computed orbits with such a kick. The kick given was that predicted by the approximate theory presented above. In the orbits shown in Fig. 4 a small betatron oscillation remains in the y plane. Exact cancellation in both planes can be achieved by trial and error.

Third, wiggler parameters should be established for use at the higher electron energies contemplated for use in synchrotron radiation facilities. To obtain x rays of the highest possible energy it will be necessary to use a helix with as short a pitch as possible. But the graph of Fig. 1 indicates that, for a pitch less than about twice the wiggler diameter, the current demands are becoming excessive. Methods for studying this problem are included in the Appendix. In particular, Eq. (A10) can be applied to establish performance on physically realizable wigglers. In practice, windings probably will be chosen of sufficient thickness that the second exponential term is of the order of about one-tenth of the first. To establish limits, however, we shall assume that the coil is infinitely thick and the second exponential vanishes. Two assumptions will be tested about achiev-

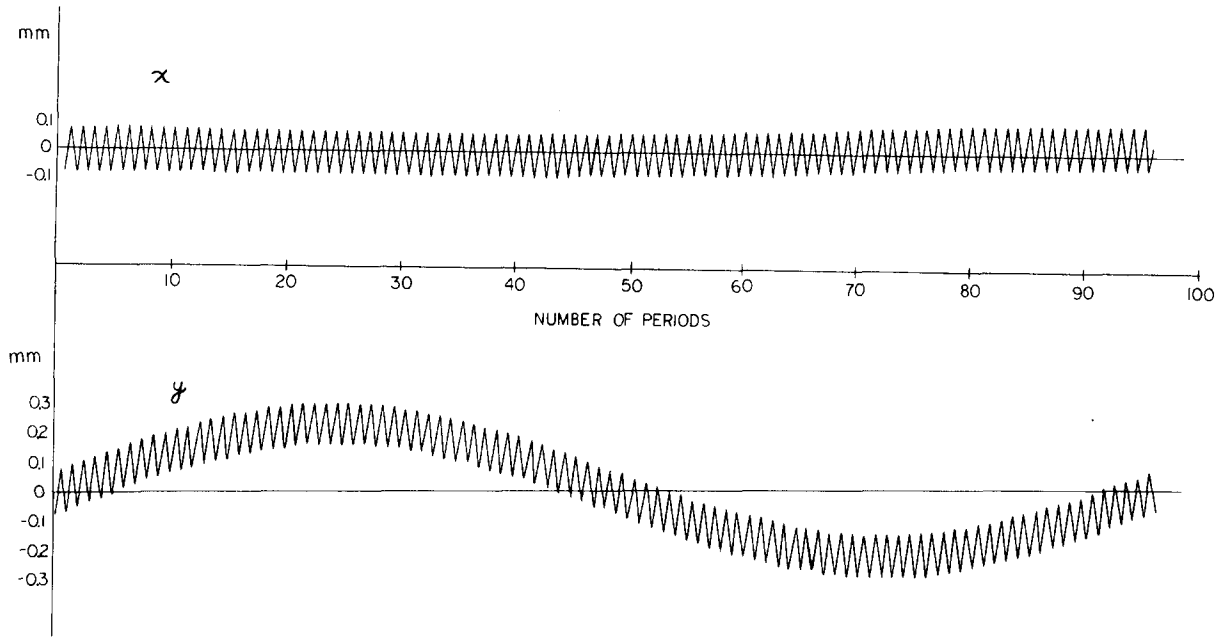

FIG. 4. Orbits with almost complete correction of the y motion.

able current density in the superconducting coil. The fields at the coil windings will be high—of the order of 50 kG for 10-kG transverse fields at the axis—and this will limit current densities for the currently available niobium-titanium wires to the order of 50 000 A/cm^2. We will then assume that developments now in progress on stranded Nb_3Sn will result soon in current densities of 100 000 A/cm^2. As a reasonable minimum value for wiggler radius we choose 0.5 cm. For these parameters, we derive from Eq. (A10) the data given in Table I.

Kincaid[4] has presented reasons for preferring to keep his parameter K close to unity. K is a dimensionless parameter which, for B_0 in gauss and λ_0 in centimeters, has the value $9.3\times10^{-5}B_0\lambda_0$. From Table I achievable parameters will be a pitch of about 2 cm and a transverse field of about 5000 G.

The cyclotron radius for 2-GeV electrons in a field of 5000 G is 11 m. The radius of the helical orbit will be about 1 μ. The peak in the emission spectrum will be at about 13 Å.

Finally, it must be shown that the effect of the wiggler is not to destroy the circulating beam in a storage ring into which it is introduced. That subject is discussed in Sec. VII.

TABLE I. Magnetic fields achievable in wigglers.

λ_0 (cm)	$B_0(I_0=50\,000$ A/cm^2) (G)	$B_0(I_0=100\,000$ A/cm^2) (G)
1	700	1400
1.5	2700	5400
2	5800	11 530
2.5	9600	19 300

VII. THE HELICAL WIGGLER IN A STORAGE RING

The helical wiggler must be matched optically if it is to be incorporated into a storage ring. This is necessary to maintain orbit stability in the ring.

Equations (9) and (10) show that for a helical wiggler of practical length ($\delta t \ll 1$) one can approximate the "smooth" transverse motion by

$$u(x_0 - r_0)\cos\omega t + (v_x/\omega)\sin\omega t, \tag{17}$$

$$v = (v_y - r_0 kc)\omega^{-1}\sin\omega t + y_0\cos\omega t. \tag{18}$$

Assuming that the wiggler is displaced horizontally by the amount r_0 and that the beam is kicked in and out to give $v_y = \pm r_0 kc$, the equilibrium orbit of the storage ring will be preserved. Using the nomenclature of Courant and Snyder,[6] the effect of the wiggler on the betatron motion can be described by simple transfer matrices:

$$M_x = M_y = \begin{bmatrix} \cos\mu_w & \beta_w\sin\mu_w \\ -\gamma_w\sin\mu_w & \cos\mu_w \end{bmatrix}, \tag{19}$$

where $\mu_w = \omega T_w = \omega L_w/c$, T_w is the passage time through the wiggler, L_w is the length of the wiggler, $\beta_w = L_w/\mu_w = c/\omega$, and $\gamma_w = 1/\beta_w$.

If the helical wiggler is inserted in a storage ring between two points 1 and 2, then, for proper matching, it is required that

$$\begin{bmatrix} \alpha_2^x \\ \beta_2^x \\ \gamma_2^x \end{bmatrix} = \begin{bmatrix} M_{11}^x M_{22}^x + M_{12}^x M_{21}^x & -M_{21}^x M_{11}^x & -M_{12}^x M_{22}^x \\ -2M_{11}^x M_{12}^x & (M_{11}^x)^2 & (M_{12}^x)^2 \\ -2M_{22}^x M_{21}^x & (M_{21}^x)^2 & (M_{22}^x)^2 \end{bmatrix} \begin{bmatrix} \alpha_1^x \\ \beta_1^x \\ \gamma_1^x \end{bmatrix} \tag{20a}$$

and

$$\begin{bmatrix} \alpha_2^y \\ \beta_2^y \\ \gamma_2^y \end{bmatrix} = \begin{bmatrix} M_{11}^y M_{22}^y + M_{12}^y M_{21}^y & -M_{21}^y M_{11}^y & -M_{12}^y M_{22}^y \\ -2M_{11}^y M_{12}^y & (M_{11}^y)^2 & (M_{12}^y)^2 \\ -2M_{22}^y M_{21}^y & (M_{21}^y)^2 & (M_{22}^y)^2 \end{bmatrix} \begin{bmatrix} \alpha_1^y \\ \beta_1^y \\ \gamma_1^y \end{bmatrix}, \tag{20b}$$

where the α's, β's, and γ's are the horizontal and vertical orbit parameters[6] of the storage ring at points 1 and 2.

Using Eq. (19), one obtains

$$\begin{bmatrix} \alpha_2^x \\ \beta_2^x \\ \gamma_2^x \end{bmatrix} = \begin{bmatrix} \cos 2\mu_w & \frac{1}{2}\beta_w^{-1} \sin 2\mu_w & -\frac{1}{2}\beta_w \sin 2\mu_w \\ -\beta_w \sin 2\mu_w & \cos^2 \mu_w & \beta_w^2 \sin^2 \mu_w \\ \beta_w^{-1} \sin 2\mu_w & \beta_w^{-2} \sin^2 \mu_w & \cos^2 \mu_w \end{bmatrix} \begin{bmatrix} \alpha_1^x \\ \beta_1^x \\ \gamma_1^x \end{bmatrix}$$

and

$$\begin{bmatrix} \alpha_2^y \\ \beta_2^y \\ \gamma_2^y \end{bmatrix} = \begin{bmatrix} \cos 2\mu_w & \frac{1}{2}\beta_w^{-1} \sin 2\mu_w & -\frac{1}{2}\beta_w \sin 2\mu_w \\ -\beta_w \sin 2\mu_w & \cos^2 \mu_w & \beta_w^2 \sin^2 \mu_w \\ \beta_w^{-1} \sin 2\mu_w & \beta_w^{-2} \sin^2 \mu_w & \cos^2 \mu_w \end{bmatrix} \begin{bmatrix} \alpha_1^y \\ \beta_1^y \\ \gamma_1^y \end{bmatrix}.$$

A reasonable location in a storage ring for a helical wiggler will be in a matched insertion. If the insertion is symmetrical (which is usually the case) and the wiggler is placed symmetrically around the insertion center, then $\alpha_2^x = -\alpha_1^x$, $\beta_2^x = \beta_1^x$, $\gamma_2^x = \gamma_1^x$, $\alpha_2^y = -\alpha_1^y$, $\beta_2^y = \beta_1^y$, $\gamma_2^y = \gamma_1^y$ and one can solve for all of the α's, β's, and γ's.

For electron energies in the GeV region and a wiggler length of a few meters, $\mu_w \ll 1$ and one can approximate the 3×3 matrix by

$$\begin{bmatrix} 1 & \mu_w/\beta_w & -L_w \\ -2L_w & 1 & 0 \\ 2\mu_w/\beta_w & 0 & 1 \end{bmatrix},$$

leading to

$$\alpha_1^x = \alpha_2^x = 0, \qquad \alpha_1^y = \alpha_2^y = 0,$$
$$\beta_1^x = \beta_2^x = \beta_w, \qquad \beta_1^y = \beta_2^y = \beta_w,$$
$$\gamma_1^x = \gamma_2^x = 1/\beta_w, \qquad \gamma_1^y = \gamma_2^y = 1/\beta_w.$$

It should be noted that $\beta_w = \sqrt{2}\rho$. For 2-GeV electrons and $B_0 = 5.5$ kG, $\rho = 12.1$ m and $\beta_w = 17.1$ m. The rms radial emittances of 2-GeV electron beams can be as low as 1.5×10^{-8} π m rad if special care is taken in the design of the storage ring.[7] One then gets an rms beam width of about 0.5 mm in the helical wiggler, and a 1-cm bore will yield an adequately long quantum lifetime. Furthermore, the horizontal angular divergence θ_r will be 3.0×10^{-5} rad. This easily satisfies the condition[4] that θ_r must be less than $(N^{1/2}\gamma)^{-1}$ to maintain spectral purity. Here N is the number of wiggler periods (of the order of 10^2).

Computer runs following orbits for 100 revolutions in a storage ring containing an optically matched helical wiggler confirm that stability can be achieved, provided the proper kicks are given to the beam at the input and output of the wiggler.

The radius of the helical path of off-momentum particles is shifted by only a very small amount, $r_0 \Delta p/p$. This makes it necessary for the local value of the momentum dispersion function of the storage ring to be zero at both ends of the wiggler. With such a configuration it can easily be shown that the effect of a helical wiggler on the relative amount of longitudinal and radial damping is negligible.

VII. CONCLUSION

An analysis has been given which yields approximate orbits of electrons in helical wigglers. There seems to be reason to expect that satisfactory performance can be achieved when the helical wiggler is incorporated in an electron storage ring. However, strong coupling between the horizontal and vertical motion in the storage ring is to be expected, resulting in increased vertical beam size. Further investigation is essential of the nonlinear effect due to helical wigglers.

ACKNOWLEDGMENTS

The authors are indebted for helpful discussions and comments to B. M. Kincaid, J. M. J. Madey, G. K. Green, R. L. Gluckstern, and H. Alan Schwettman.

APPENDIX: MAGNETIC FIELD PATTERNS AND CURRENT DISTRIBUTION

It will be assumed that the field has a sinusoidal distribution in the axial direction, the distribution having the same period as the helical winding. It will be assumed further that no higher harmonics are present. The field pattern can then be represented by

$$B_r = F(r) \sin(\theta - kz),$$
$$B_\theta = G(r) \cos(\theta - kz),$$

where $2\pi/k$ is the axial distance in which the field makes a complete revolution. Substitution of these expressions in Maxwell's equations and elimination of B_z by second differentiation reveals the fact that rG is proportional to $I_1(kr)$, a first-order Bessel function of imaginary argument. Finally, we obtain

$$\begin{aligned} B_r &= 2B_0[I_0(kr) - (1/kr)I_1(kr)] \sin(\theta - kz), \\ B_\theta &= (2B_0/kr)I_1(kr) \cos(\theta - kz), \\ B_z &= -2B_0 I_1(kr) \cos(\theta - kz), \end{aligned} \tag{A1}$$

where B_0 is the transverse field amplitude at the axis of the helical winding.

Near the axis the fields can be represented by approximate expressions using the leading terms in the series representing the Bessel functions. For kr less than about 0.8, the field components can be represented with errors less than 1% by

$$\begin{aligned} B_r &= B_0(1 + \tfrac{3}{8}k^2r^2) \sin(\theta - kz), \\ B_\theta &= B_0(1 + \tfrac{1}{8}k^2r^2) \cos(\theta - kz), \\ B_z &= -kB_0 r(1 + \tfrac{1}{8}k^2r^2) \cos(\theta - kz). \end{aligned} \tag{A2}$$

In rectangular coordinates the field components are

$$B_x = -B_0\{[1+\tfrac{1}{8}k^2(3x^2+y^2)]\sin kz - (\tfrac{1}{4}k^2xy)\cos kz\},$$
$$B_y = B_0\{[1+\tfrac{1}{8}k^2(x^2+3y^2)]\cos kz - (\tfrac{1}{4}k^2xy)\sin kz\}, \quad \text{(A3)}$$
$$B_z = -B_0[1+\tfrac{1}{8}k^2(x^2+y^2)](x\cos kz + y\sin kz).$$

Outside of the helical winding the field expressions will be similar, but, in order that the fields vanish at infinity, it will be necessary to replace the I functions with K functions. The field amplitude outside will be obtained by matching the radial component of B. This will introduce into all components a factor

$$A = \frac{\pi I_0(ka) - (1/ka)I_1(ka)}{2K_0(ka) + (1/ka)K_1(ka)}, \quad \text{(A4)}$$

where a is the radius of the winding which, for the moment, we assume to be infinitesimal in thickness.

The current distribution can be derived from the discontinuity in B_θ and B_z

$$I_\theta = -\frac{2B_0}{4\pi\mu_0}\left(\frac{2A}{\pi}K_1(ka) + I_1(ka)\right)\cos(\theta - kz),$$
$$I_z = \frac{2B_0}{4\pi\mu_0 ka}\left(\frac{2}{\pi}K_1(ka) + I_1(ka)\right)\cos(\theta - kz). \quad \text{(A5)}$$

The total current is, with the Wronskian relation,

$$I = \frac{5B_0}{\pi}\frac{(1+1/k^2a^2)^{1/2}}{kaK_0(ka) + K_1(ka)}\cos(\theta - kz). \quad \text{(A6)}$$

Here I is given in A cm^{-1} (axial) and B_0 is in G. The total current in one turn of the helix will be given by setting $\theta = 0$ and by integrating Eq. (A6) from $kz = -\frac{1}{2}\pi$ to $+\frac{1}{2}\pi$ to obtain

$$I_{\text{tot}} = \frac{5\lambda_0 B_0}{\pi^2}\frac{(1+1/k^2a^2)^{1/2}}{kaK_0(ka) + K_1(ka)}, \quad \text{(A7)}$$

where λ_0 $(= 2\pi/k)$ is the pitch of each helix in cm.

Equation (A7) is to be compared with Kincaid's Eq. (1). The two expressions differ by a factor $(4/\pi)(1+1/k^2a^2)^{1/2}$; this small difference is attributable to the fact that this treatment relates to a distributed winding, whereas Kincaid's helices are single wires of infinitesimal cross section.

Equation (A7) is plotted in a semilog plot in Fig. 1. It is evident from the plot that, above $a/\lambda_0 = 0.2$, the expression for $I_{\text{tot}}/\lambda_0 B_0$ can be represented by an exponential:

$$I_{\text{tot}}/\lambda_0 B_0 = 0.246\exp(5.68a/\lambda_0) \quad (\text{A cm}^{-1}\,\text{G}^{-1}). \quad \text{(A8)}$$

Using expression (A8) it is possible to analyze windings of finite thickness. We assume that the axially sinusoidal current distribution is replaced by a block of current of uniform density, I_0 (A/cm^2), and of axial width $\frac{1}{3}\lambda_0$. Near the axis, this will give fields which are to a good approximation the same as those provided by the sinusoidal distribution.

The total current in a block of infinitesimal thickness da at radius a will be $I_0(\frac{1}{3}\lambda_0)\,da$; it will provide a transverse field dB_0 on the axis given by Eq. (A8)

$$dB_0 = 1.355 I_0\exp(-5.68\ a/\lambda_0)\,da. \quad \text{(A9)}$$

For a coil of finite thickness, having inner and outer radii a_1 and a_2, we integrate Eq. (A9) to obtain

$$B_0 = 0.2385 I_0\lambda_0[\exp(-5.68a_1/\lambda_0) - \exp(-5.68a_2/\lambda_0)](\text{G}). \quad \text{(A10)}$$

For coils having a_1/λ_0 greater than 0.2, Eq. (A10) can be used to establish the current density I_0 in A cm^{-2} required to produce a transverse magnetic flux density of B_0 (G) in a helix of given pitch and inner and outer dimensions.

*Work performed under the auspices of the Energy Research and Development Administration.

[1]Luis R. Elias, William M. Fairbank, John M. J. Madey, H. Alan Schwettman, and Todd I. Smith, Phys. Rev. Lett. **36**, 717 (1976).
[2]H. Motz, J. Appl. Phys. **22**, 527 (1951); **24**, 826 (1953).
[3]John M. J. Madey, J. Appl. Phys. **42**, 1906 (1971).
[4]Brian M. Kincaid, preceding paper, J. Appl. Phys. **48**, xxx (1977).
[5]W. R. Smythe, *Static and Dynamic Electricity* (McGraw-Hill, New York, 1950), p. 277.
[6]E. D. Courant and H. S. Snyder, Ann. Phys. **3**, 1 (1958).
[7]Brookhaven National Laboratory Report BNL 50595, 1977 (unpublished).